SCIENTIFIC REPORTS

OPEN

SUBJECT AREAS:
MATERIALS FOR ENERGY AND CATALYSIS
INORGANIC CHEMISTRY
OPTICAL MATERIALS
NANOWIRES

Received
23 April 2013

Accepted
26 July 2013

Published
14 August 2013

Correspondence and requests for materials should be addressed to J.L.W. (jlwang@ntu.edu.sg)

General Route to ZnO Nanorod Arrays on Conducting Substrates via Galvanic-cell-based approach

Zhaoke Zheng, Zhi Shiuh Lim, Yuan Peng, Lu You, Lang Chen & Junling Wang

School of Materials Science and Engineering, Nanyang Technological University, Singapore, 639798.

Wurtzite ZnO nanorod exhibits many unique properties, which make it promising for various optoelectronic applications. To grow well-aligned ZnO nanorod arrays on various substrates, a seed layer is usually required to improve the density and vertical alignment. The reported works about seedless hydrothermal synthesis either require special substrates, or require external electrical field to enhance the ZnO nucleation. Here, we report a general method for the one-pot synthesis of homogenous and well-aligned ZnO nanorods on common conducting substrates without a seed layer. This method, based on the galvanic-cell structure, makes use of the contact potential between different materials as the driving force for ZnO growth. It is applicable to different conducting substrates at low temperature. More importantly, the as-grown ZnO nanorods show enhanced photoelectric response. This unique large scale low-temperature processing method could be of great importance for the application of ZnO nanostructures.

One-dimensional semiconductor nanostructures, which display enhanced optical and electrical properties, have attracted much attention due to their potential applications in next generation electronic and photonic devices[1–5]. Controlled growth of one-dimensional nanostructures on various substrates is highly desirable. Among them, wurtzite ZnO is of particular interest because of its direct wide band gap (3.37 eV) and large exciton binding energy (60 meV), which make it promising for various optoelectronic applications[6–10]. There have been extensive studies on different approaches to synthesize well-aligned ZnO nanorod arrays, e.g. chemical vapor deposition (CVD)[11], vapor-liquid-solid deposition[12,13], pulse laser deposition (PLD)[14], and solution-based growth methods[15,16]. Among them, vapor-phase deposition usually requires single-crystal substrates and high growth temperature, which is incompatible with the low-cost conducting substrates widely used for optoelectronic devices.

Solution-based methods are especially attractive for industry because of the low-cost, low-processing temperature, environmental friendliness, and ease of morphology control[17,18]. To grow ZnO nanorods on various substrates, a seed layer is usually required to improve the density and vertical alignment of the nanorods[19–21]. The seed layer, composed of packed ZnO nanocrystals acting as homoepitaxial nucleation sites, is generally prepared by sol-gel or sputtering method. Annealing at high temperature is required to ensure seed particles generation and adhesion to the substrate, which diminishes the advantage of low-temperature solution growth methods. To date, several works have reported the seedless hydrothermal synthesis of ZnO nanorod arrays. However, they either require expensive single-crystal substrates (e.g. Al_2O_3 and GaN[22–25]) or special substrate (e.g. Ti/Au deposited substrate[26,27] and cover glass[28]), or an external electrical field to enhance the ZnO nucleation[29,30]. Therefore, a general seedless approach for the synthesis of well-aligned ZnO nanorod arrays on various substrates is still desirable.

Here, we reported a novel galvanic-cell-based approach towards the direct growth of ZnO nanorod arrays on various conducting substrates at low temperature without the seed layer. This approach is simple and the mechanism is described for the first time. The growth is substrate-independent and can be realized on different conducting materials regardless of the surface roughness, crystallinity, or lattice structure. The substrates that have been tested include Pt and Au-coated silicon wafers, transparent conducting oxides such as fluorine-doped tin oxide (FTO) and indium tin oxide (ITO), and oxide-free copper plate. Furthermore, the as-grown ZnO nanorods show enhanced photoelectric response compared with those grown with a ZnO seed layer, which is likely due to the more efficient charge transport directly from nanorods to the conducting substrates.

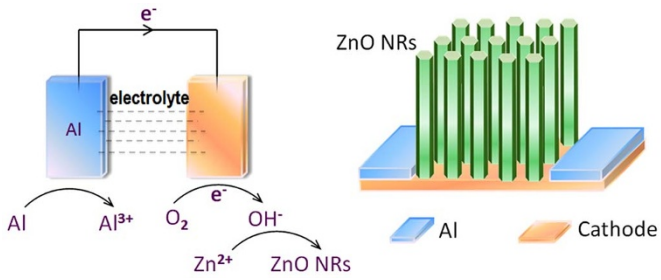

Figure 1 | Schematic illustration of the galvanic cell based fabrication process of ZnO nanorod arrays. Al is used as the sacrificing anode and ZnO growth occurs on the cathode substrate.

Results

Contact potential driven ZnO nanorods growth. The approach proposed is based on the galvanic cell structure, which is schematically shown in Figure 1. The ZnO growth mechanism is similar to that of the electrochemical deposition, except that a galvanic cell is employed instead of an external power source. The work function difference between the two materials, one of which being the substrate for ZnO growth, creates a bias that drives the reactions indicated in Figure 1. In our study, Al was used as the sacrificing anode, while the relatively inert substrate (Pt or Au-coated silicon, Cu, FTO and ITO) as the cathode. The edge of the substrate was covered with Al to make a direct contact between the anode and cathode. The reduction potential for Al is more negative than that of the inert cathode. Thus, Al will lose electrons to develop a positive charge, and the electron will transfer to the cathode substrate. The electrolyte is an aqueous solution containing zinc nitrate hexahydrate and hexamethylenetetramine, and its pH is close to neutral (~6.1). Reduction reaction of dissolved oxygen occur on the cathode substrate ($O_2 + 2H_2O + 4\ e^- \rightarrow 4OH^-$), followed by the formation of $Zn(OH)_2$ and dehydration to form ZnO.

When using Pt-coated silicon wafers (Pt/Si) as the cathode substrate, well-aligned single-crystal hexagonal nanorods of ~250 nm in diameter grow homogeneously on the Pt surface (Figure 2a, c and Figure S1). From the field emission scanning electron microscopy (FESEM) image taken at a 30° angle, we can see that these nanorods grow perpendicular to the substrate surface. X-ray diffraction (XRD) reveals a wurtzite structure with an enhanced (002) peak resulting from the preferred c-axis orientation of the ZnO nanorods. It was noted that the Pt/Si substrate contains grains of ~60 nm (see AFM image in Figure S2), which is totally different from the ZnO nanorod dimension. This indicates that the growth of nanorods is not facilitated by topography features. We have also tried hydrothermal growth of ZnO on Pt/Si substrate without the Al at the edge. As shown in Figure 1e, only several randomly dispersed ZnO microrods with diameter of ~2.5 μm and length of ~20 μm were observed, which confirms the vital role of Al.

To clarify the chemical reaction occurs at the Al anode, the product generated at the Al region was investigated. Figure 2d shows the FESEM image and EDS result. The as-grown product is micro-sized sheets interconnected with each other, and its XRD pattern cannot be indexed to any phase of oxides (Figure S3). However, EDS analysis shows that this product is composed of Al, Zn, and O with the atomic ratio of 1 : 2.3 : 8.1. The ratio of [O]/[metal] is higher than that of the corresponding oxides. To further investigate the composition of the product generated at the Al region, the sintering experiment was carried out. After being annealed at 350 °C in air, the micro-sized sheets collapsed to form larger sheets (Figure S4), while the atomic ratio of Al, Zn, and O changed to 1 : 2.3 : 5.2. Considering the fact that XRD pattern after annealing shows wurtzite ZnO peaks, we conclude that the products on Al region are mainly hydroxides of Al and Zn. The FTIR spectroscopy (Figure S5) further verifies our conjecture. The broad absorption peaks at 3405 cm^{-1} and 1639 cm^{-1} were assigned to the stretching and bending modes of OH groups, respectively[31]. After annealing, the intensity of the OH peaks becomes much lower, which is due to the dehydration of OH groups. In short, the sacrificing anode, metallic Al, loses electrons to form Al cations, followed by the formation of hydroxide mixture.

Generality of the approach and nanorod growth sequence. To investigate the generality of our galvanic cell based synthesis of ZnO nanorods, several other conducting substrates were tested, including Au-coated silicon wafer, transparent FTO glass and Cu

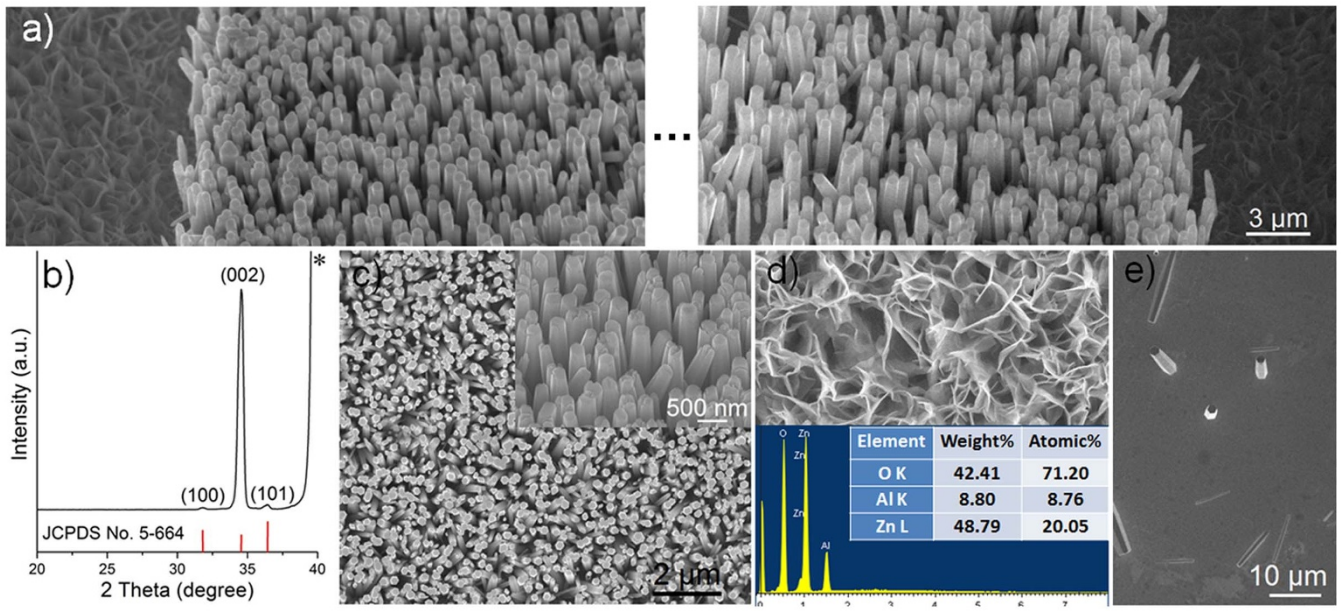

Figure 2 | FESEM images and XRD patterns of ZnO nanorods grown on Pt-coated silicon wafers. (a, c) FESEM images and (b) XRD patterns of ZnO nanorod arrays grown on Pt-coated silicon wafers (Pt/Si) with Al on the edge. The peaks marked with asterisks are associated with the substrate. (d) FESEM images and EDS of the product grown on Al region. (e) FESEM images of ZnO nanorod grown on Pt/Si without Al.

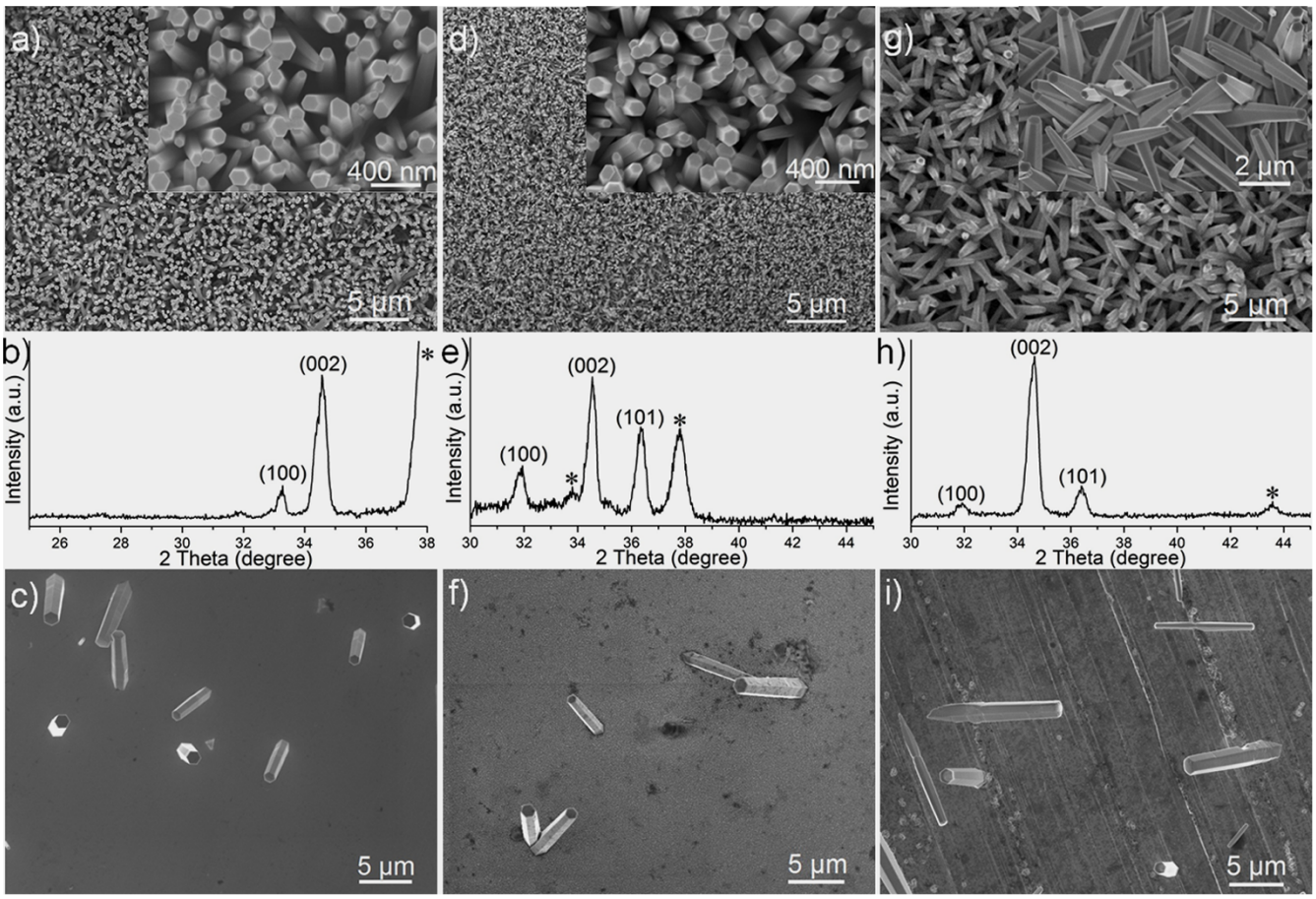

Figure 3 | FESEM images and XRD patterns of ZnO nanorod arrays grown on different substrates with/without Al coving the edges. (a–b) Au-coated silicon wafer, (d–e) FTO glass, (g–h) Cu plate. The peaks marked with asterisks are associated with the substrates. (c, f, i) FESEM images of ZnO nanorod grown on corresponding substrates without Al.

plate (Figure 3). For all three substrates with Al attached to the edge, we can see dense ZnO nanorods grow homogeneously on the surface. XRD patterns for these samples all show wurtzite ZnO with an enhanced (002) peak. On the other hand, in the absence of Al, we can only find several randomly dispersed ZnO microrods on the surface (Figure 3c, f, i). Among the substrates we have tested, growth of ZnO nanorod arrays on common transparent substrates, such as FTO and ITO glasses, is of great importance for applications in photoelectronic devices. Homogeneous ZnO nanorod arrays can be obtained on such substrates at large scale using this method (Figure 3d and Figure S6). Furthermore, the sample remains semi-transparent after the ZnO growth as shown in Figure S7.

In order to study the initial nucleation and subsequent growth of ZnO nanorods, time dependent characterization was conducted for the sample on Cu plate (Figure S8). After 30 min of reaction, we observe that hexagonal ZnO nano-plates of ~300 nm in diameter grow homogeneously on the substrate. This is different from typical solution-based ZnO nanorod growth where small-size nanorods with diameter of ~50 nm and length of 0.5 μm can be formed in the initial stage[32]. In our cases, the negatively charged cathode will attract zinc cations and result in the lateral growth of nano-plates in the nucleation process. When the reaction time increases to 4 h, the diameter of ZnO nanorods only increases slightly to 400 nm while the length of nanorods increases significantly. The metastable polar (001) plane has higher surface energy than the other "low-symmetry" nonpolar planes, which leads to the anisotropic growth of the crystal along the [001] direction. To conclude, the role of the galvanic cell structure is to initiate ZnO nucleation on the cathode surface, and the subsequent growth process is controlled by the anisotropy of ZnO crystal.

Controlled growth of ZnO nanorods on complex patterns. Besides large scale low temperature synthesis without a seed layer, another advantage of this technique is that it enables selective growth of ZnO nanorods on different patterns. As a demonstration, we have prepared different patterns of the inert cathode, Pt or Cu, on Al substrate using PLD following standard photolithography process. After hydrothermal growth, vertically aligned ZnO nanorods were only observed on the Pt or Cu region (Figure 4 and Figure S9–11), and these ZnO arrays exhibit a clear edge which is consistent with the profile of the Pt or Cu pattern. It clearly demonstrates that this method can be used for the controlled growth of ZnO nanorods on sophisticated patterns.

To assess the quality of the obtained ZnO nanorods, we conducted room temperature photoluminescence (PL) measurements on the nanorods grown on FTO and ITO glasses (Figure 5a). An UV emission peak around 393 nm (~3.16 eV) was observed. The UV peak is attributed to the near-band-edge emission, namely the recombination of free excitons between conduction band and valence band[33,34], which is consistent with values reported for ZnO prepared by hydrothermal (3.12–3.29 eV)[35,36] and electrodeposition (3.12–3.30 eV) methods[37,38]. Normally a broad visible light emission centered around 620 nm can be found in electrochemically and hydrothermally grown ZnO[39]. This orange-red emission is attributed to radiative transitions involving defect-induced energy levels located in the band gap, and is assumed to involve interstitial oxygen ions (O_i).

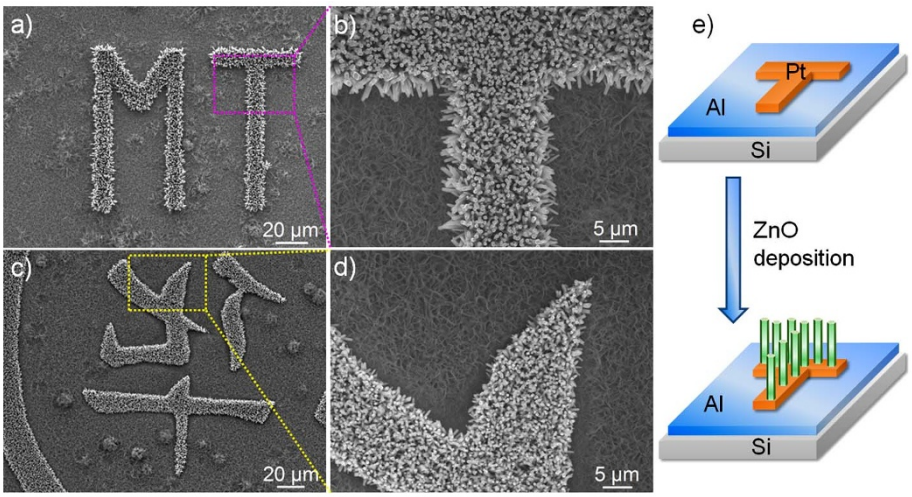

Figure 4 | Selective growth of ZnO nanorods on complex patterns. (a–d) FESEM images and (e) schematic representation of ZnO nanorods grown on different Pt patterns which are deposited on Al substrate by PLD.

However, our samples do not display such orange-red emission, which indicates the high optical quality and low defects density of the as-grown ZnO nanorods[40].

Discussion

These high quality ZnO nanorods, which are grown directly on conductive substrates without the polycrystalline ZnO seed layer, are expected to possess improved photoelectric performance. Figure 5b shows the *J–V* curves of ZnO nanorods grown on FTO using our method (ZnO/FTO) in dark and under illumination. For comparison, the *J–V* curves of ZnO nanorod arrays grown with polycrystalline ZnO seed layer (ZnO/Seed/FTO), which prepared by zinc acetate deposition[19], were also tested. The ZnO/FTO sampleexhibits a significantly enhanced (52% increase in photocurrent at 0.7 V) photoelectric response compared with ZnO/Seed/FTO. By removing the polycrystalline seed layer, we have eliminated the recombination centers for photo-generated carriers and enhanced the charge transport from ZnO nanorods to the substrate.

In summary, we have developed a general method for the one-pot synthesis of homogenous and well-aligned ZnO nanorods on common conducting substrates. This method, based on the galvanic cell structure, offers several advantages over conventional routes. First, it is substrate-independent and can be realized on various conducting substrates regardless of their surface roughness or crystal structure. Second, in comparison with conventional seed layer-mediated growth, it is facile and economical, as no annealing or vacuum process is needed for the seed layer preparation. This method can also be used for the controlled growth of ZnO nanorods on sophisticated patterns. More importantly, the as-grown ZnO nanorods show enhanced photoelectric response compared with those grown with seed layer, which is likely due to the efficient charge transport directly from nanorods to conducting substrates. This unique low-temperature processing method could be of great importance for the application of ZnO nanorods.

Methods

Materials. Zinc nitrate hexahydrate ($Zn(NO_3)_2{\cdot}6H_2O$), hexamethylenetetramine (HMTA $C_6H_{12}N_4$) were purchased from Sigma Aldrich. All the chemicals were used as received without further purification. Pt-coated (~200 nm) silicon wafers (Pt/Si), Au-coated (~50 nm) silicon wafers (Au/Si) were purchased from MTI Corporation. Cu plates (99.9%) were purchased from Alfa Aesar.

Substrate Preparation. Pt/Si wafers, Au/Si wafers, Cu plates, fluorine-doped tin oxide (FTO) and indium tin oxide (ITO) glasses were cleaned ultrasonically with acetone and ethanol for 10 min, respectively, and then dried with nitrogen before ZnO growth.

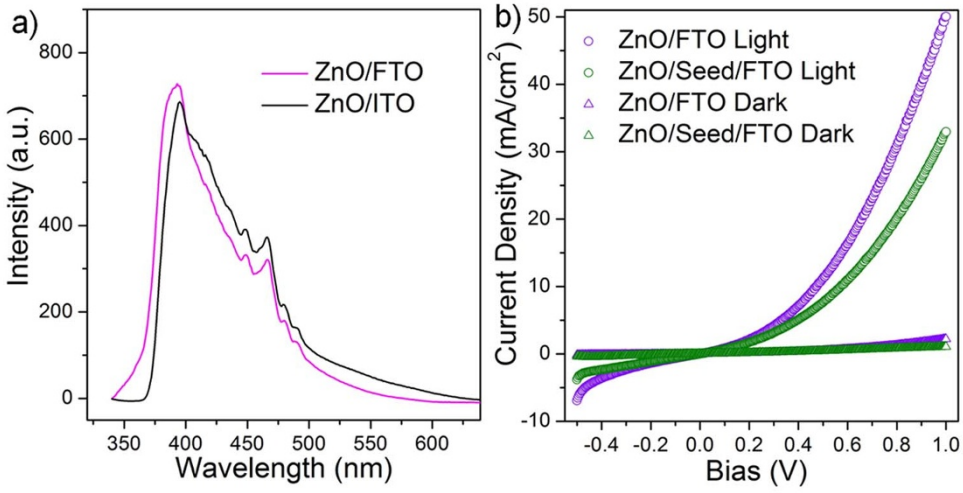

Figure 5 | Photoelectric Properties of ZnO nanorods arrays. (a) Photo luminescence spectra of ZnO nanorods grown on FTO and ITO glasses with Al covering the edge. (b) *J–V* curves of ZnO nanorods grown on FTO with Al or with ZnO seed layer in darkness and under illumination.

Attaching Al on Cathode Substrate. The Al was loaded on the cathode substrate in two ways: (1) For the large-scale growth of ZnO nanorods on these substrates, the edge of the substrate was simply covered by Al foil, and the exposed substrate can be used for the growth of ZnO nanorods. (2) For the controlled growth of ZnO nanorods on complex patterns, Al was selectively deposited on the cathode substrate by PLD. Pt and Cu patterns were also deposited on Al substrate by PLD. For method (2), the distance between the metal target and the substrate was ~50 mm. The vacuum chamber was evacuated to a base pressure of 1×10^{-5} Pa. The energy at the target surface and repetition rate of the laser was 100 mJ and 10 Hz, respectively.

Hydrothermal Growth of ZnO Nanorods. Hydrothermal ZnO growth was carried out by suspending the above-mentioned substrates upside-down in an aqueous solution containing 25 mM zinc nitrate hexahydrate and 25 mM hexamethylenetetramine at 90 °C[32]. The typical growth time is 4 hours. The samples were then removed from solution, rinsed with deionized water, and dried at 50 °C.

Characterization. X-ray diffraction patterns were obtained using a Shimadzu XRD-6000 X-ray diffractometer with Cu Kα radiation (λ = 1.5418 Å). Field emission scanning electron microscopy images were obtained using a JSM-7600F microscope. The EDS was taken on an OXFORD INCA X-Max Energy Dispersive X-Ray Spectroscopy. Surface topography measurements were conducted using a commercial atomic force microscope system (Asylum Research MFP-3D) with DPE probe (Mikromash, spring constant ~2 N/m). The Fourier Transform Infrared absorption spectra were carried out on PerkinElmer Frontier FTIR/NIR Spectrometer (USA) over the range of 500–4000 cm^{-1}. The fluorescence spectra were obtained on a Shimadzu/RF-5301PC fluorescence spectrometer (Japan) at room temperature. *J–V* measurements were performed using a Keithley 2400 SourceMeter with a custom-made LabTracer program. A 300 W Xenon Arc Lamp (Newport) with appropriate filter was used as the light source. Au contacts (small square 0.03 cm^2) were evaporated onto the ZnO using a Vacuum Evaporator (JEOL JEE-420) through a patterned shadow mask under high vacuum ($<10^{-5}$ Torr).

1. Hochbaum, A. I. & Yang, P. Semiconductor nanowires for energy conversion. *Chem. Rev.* **110**, 527–546 (2010).
2. Iijima, S. Helical microtubules of graphitic carbon. *Nature* **354**, 56–58 (1991).
3. Law, M., Greene, L. E., Johnson, J. C., Saykally, R. & Yang, P. Nanowire dye-sensitized solar cells. *Nat. Mater.* **4**, 455–459 (2005).
4. Zheng, Z. K. *et al.* Hydrogenated titania: synergy of surface modification and morphology improvement for enhanced photocatalytic activity. *Chem. Commun.* **48**, 5733–5735 (2012).
5. Zheng, Z. K., Huang, B. B., Qin, X. Y., Zhang, X. Y. & Dai, Y. Strategic Synthesis of Hierarchical TiO_2 Microspheres with Enhanced Photocatalytic Activity. *Chem. Eur. J.* **16**, 11266–11270 (2010).
6. Ahsanulhaq, Q., Kim, J. H. & Hahn, Y. B. Controlled selective growth of ZnO nanorod arrays and their field emission properties. *Nanotechnology* **18**, 485307–485312 (2007).
7. Xu, C. K., Wu, J. M., Desai, U. V. & Gao, D. Multilayer assembly of nanowire arrays for dye-sensitized solar cells. *J. Am. Chem. Soc.* **133**, 8122–8125 (2011).
8. Sun, X. W. & Wang, J. X. Fast switching electrochromic display using a viologen-modified ZnO nanowire array electrode. *Nano Lett.* **8**, 1884–1889 (2008).
9. Wang, X. D. *et al.* Piezoelectric field effect transistor and nanoforce sensor based on a single ZnO nanowire. *Nano Lett.* **6**, 2768–2772 (2006).
10. Lee, S. W., Jeong, M. C. & Myoung, J. M. Magnetic alignment of ZnO nanowires for optoelectronic device applications. *Appl. Phys. Lett.* **90**, 133115-1–133115-3 (2007).
11. Wu, J. J. & Liu, S. C. Low-temperature growth of well-aligned ZnO nanorods by chemical vapor deposition. *Adv. Mater.* **14**, 215–218 (2002).
12. Gao, P. & Wang, Z. L. Self-assembled nanowire-nanoribbon junction arrays of ZnO. *J. Phys. Chem. B* **106**, 12653–12658 (2002).
13. Wang, S. *et al.* Growth of uniformly aligned ZnO nanowire heterojunction arrays on GaN, AlN, and $Al_{0.5}Ga_{0.5}N$ substrates. *J. Am. Chem. Soc.* **127**, 7920–7923 (2005).
14. Choi, J. H., Tabata, H. & Kawai, T. Initial preferred growth in zinc oxide thin films on Si and amorphous substrates by a pulsed laser deposition. *J. Cryst. Growth* **226**, 493–500 (2001).
15. Vayssieres, L. Growth of arrayed nanorods and nanowires of ZnO from aqueous solutions. *Adv. Mater.* **15**, 464–466 (2003).
16. Peulon, S. & Lincot, D. Cathodic electrodeposition from aqueous solution of dense or open-structured zinc oxide films. *Adv. Mater.* **8**, 166–170 (1996).
17. Kim, J. H., Andeen, D. & Lange, F. F. Hydrothermal Growth of Periodic, Single-crystal ZnO microrods and microtunnels. *Adv. Mater.* **18**, 2453–2457 (2006).
18. Das, S. K., Sahoo, S. N., Sarangi, S. N. & Sahoo, P. K. Substrate effect of hydrothermally grown ZnO nanorods and its luminescence properties. *J. Exp. Nanosci.* **8**, 382–388 (2012).
19. Greene, L. E. *et al.* General route to vertical ZnO nanowire arrays using textured ZnO seeds. *Nano Lett.* **5**, 1231–1236 (2005).
20. Anthony, S. P., Lee, J. I. & Kim, J. K. Tuning optical band gap of vertically aligned ZnO nanowire arrays grown by homoepitaxial electrodeposition. *Appl. Phys. Lett.* **90**, 103107–103109 (2007).
21. Holloway, T., Mundle, R., Dondapati, H., Bahoura, M. & Pradhan, A. K. Aligned Al:ZnO nanorods on Si with different barrier layers for optoelectronic applications. *Chem. Phys. Lett.* **534**, 48–53 (2012).
22. Pauporte, Th. & Lincot, D. Heteroepitaxial electrodeposition of zinc oxide films on gallium nitride. *Appl. Phys. Lett.* **75**, 3817–3819 (1999).
23. Kim, J. H., Andeen, D. & Lange, F. F. Hydrothermal growth of periodic, single-crystal ZnO microrods and microtunnels. *Adv. Mater.* **18**, 2453–2457 (2006).
24. Ng, H. T. *et al.* Single crystal nanowire vertical surround-gate field-effect transistor. *Nano Lett.* **4**, 1247–1252 (2004).
25. Fan, H. J. *et al.* Patterned growth of aligned ZnO nanowire arrays on sapphire and GaN layers. *Superlattices Microstruct.* **36**, 95–105 (2004).
26. Tian, J. H. *et al.* Improved seedless hydrothermal synthesis of dense and ultralong ZnO nanowires. *Nanotechnology* **22**, 245601 (2011).
27. Xu, S., Lao, C. S., Weintraub, B. & Wang, Z. L. Density-controlled growth of aligned ZnO nanowire arrays by seedless chemical approach on smooth surfaces. *J. Mater. Res.* **23**, 2072–2077 (2008).
28. Ahsanulhaq, Q., Kim, J. H., Kim, J. H. & Hahn, Y. B. Seedless pattern growth of quasi-aligned ZnO nanorod arrays on cover glass substrates in solution. *Nanoscale Res. Lett.* **5**, 669–674 (2010).
29. Weintraub, B., Deng, Y. L. & Wang, Z. L. Position-controlled seedless growth of ZnO nanorod arrays on a polymer substrate via wet chemical synthesis. *J. Phys. Chem. C* **111**, 10162–10165 (2007).
30. Choi, H. W., Lee, K. S. & Alford, T. L. Optimization of antireflective zinc oxide nanorod arrays on seedless substrate for bulk-heterojunction organic solar cells. *Appl. Phys. Lett.* **101**, 153301 (2012).
31. Costenaro, D., Carniato, F., Gatti, G., Bisio, C. & Marchese, L. On the physico-chemical properties of ZnO nanosheets modified with luminescent CdTe nanocrystals. *J. Phys. Chem. C* **115**, 25257–25265 (2011).
32. Greene, L. E. *et al.* Low-temperature wafer-scale production of ZnO nanowire arrays. *Angew. Chem., Int. Ed.* **42**, 3031–3034 (2003).
33. Yang, F. *et al.* Controllable low temperature vapor-solid growth and hexagonal disk enhanced field emission property of ZnO nanorod arrays and hexagonal nanodisk networks. *ACS Appl. Mater. Interfaces* **4**, 3852–3859 (2012).
34. Kong, Y. C., Yu, D. P., Zhang, B., Fang, W. & Feng, S. Q. Ultraviolet-emitting ZnO nanowires synthesized by a physical vapor deposition approach. *Appl. Phys. Lett.* **78**, 407–409 (2001).
35. Le, H. Q., Chua, S. J., Koh, Y. W., Loh, K. P. & Fitzgerald, E. A. Systematic studies of the epitaxial growth of single-crystal ZnO nanorods on GaN using hydrothermal synthesis. *J. Cryst. Growth* **293**, 36–42 (2006).
36. Xu, F., Lu, Y., Xie, Y. & Liu, Y. Synthesis and photoluminescence of assembly-controlled ZnO architectures by aqueous chemical growth. *J. Phys. Chem. C* **113**, 1052–1059 (2009).
37. Izaki, M., Shinagawa, T. & Takahashi, H. Room temperature ultraviolet light emitting ZnO layer prepared by low-temperature electrodeposition. *J. Phys. D: Appl. Phys.* **39**, 1481–1484 (2006).
38. Pauporte, T., Jouanno, E., Pelle, F., Viana, B. & Aschehoug, P. Key growth parameters for the electrodeposition of ZnO films with an intense UV-Light emission at room temperature. *J. Phys. Chem. C* **113**, 10422–10431 (2009).
39. Liu, M., Kitai, H. & Mascher, P. Point defects and luminescence centres in zinc oxide and zinc oxide doped with manganese. *J. Lumin.* **54**, 35–42 (1992).
40. Chen, L. Y. & Yin, Y. T. Facile Continuous Flow Injection Process for High Quality Long ZnO Nanowire Arrays Synthesis. *Cryst.Growth Des.* **12**, 1055–1059 (2012).

Acknowledgements

This work is supported by National Research Foundation of Singapore under project NRF-CRP5-2009-04.

Author contributions

J.W. supervised the whole project. Z.Z. designed, preformed the experiments and wrote the paper. Y.P. and Z.L. performed the SEM characterization and photolithography. L.Y. performed the AFM characterization. L.C. and J.W. revised the manuscript. All authors analyzed and discussed the experimental results.

Additional information

Supplementary information accompanies this paper at http://www.nature.com/scientificreports

Competing financial interests: The authors declare no competing financial interests.

How to cite this article: Zheng, Z.K. *et al.* General Route to ZnO Nanorod Arrays on Conducting Substrates via Galvanic-cell-based approach. *Sci. Rep.* **3**, 2434; DOI:10.1038/srep02434 (2013).